Taylor & Francis
Taylor & Francis Group

Phase Transitions

A Multinational Journal

ISSN: 0141-1594 (Print) 1029-0338 (Online) Journal homepage: http://www.tandfonline.com/loi/gpht20

Antibiotic loading and release studies of LSMO nanoparticles embedded in an acrylic polymer

Sonali Biswas, Sunita Keshri, Sudipta Goswami, Jinu Isaac, Swastika Ganguly & Nikolai Perov

PHASE TRANSITIONS, 2016
http://dx.doi.org/10.1080/01411594.2016.1156681

Taylor & Francis
Taylor & Francis Group

Antibiotic loading and release studies of LSMO nanoparticles embedded in an acrylic polymer

Sonali Biswas[a], Sunita Keshri[a], Sudipta Goswami[b], Jinu Isaac[c], Swastika Ganguly[c] and Nikolai Perov[d]

[a]Department of Physics, Birla Institute of Technology, Mesra, Ranchi, India; [b]Department of Chemical Engineering and Technology, Birla Institute of Technology, Mesra, Ranchi, India; [c]Department of Pharmaceutical Science and Technology, Birla Institute of Technology, Mesra, Ranchi, India; [d]Department of Physics, Lomonosov Moscow State University, Moscow, Russian Federation

ABSTRACT
In this paper, we present the drug loading and release works of $La_{0.67}Sr_{0.33}MnO_3$ (LSMO) manganite nanoparticles (NPs). The LSMO NPs, grown using the sol–gel method, were embedded in an acrylic interpenetrating polymer network to make the sample applicable for biomedical purposes. The results of scanning electron microscopy showed that these NPs were well dispersed in the polymer. The grain size of these NPs lies in the range of 25–45 nm, as confirmed by transmission electron microscopy. The measurements of DC magnetization and hysteresis loops reveal that the basic magnetic behaviour of the LSMO NPs remained almost unaltered even after embedding in polymer, but with lower saturation value of magnetization. The drug loading and release studies of the grown sample were carried out using an antibiotic, ciprofloxacin. The minimum inhibitory effect of the sample loaded with this drug has exhibited high activity against different strains of bacteria, comparable to the pure ciprofloxacin.

ARTICLE HISTORY
Received 1 August 2015
Accepted 10 February 2016

KEYWORDS
Manganite; nanoparticles; magnetization; biomedical applications

1. Introduction

In recent years, an increasing interest has been paid to the application of magnetic nanoparticles (NPs) in biomedicine and bioengineering, including magnetically activated drug delivery,[1] bioseparation,[2] magnetic resonance imaging [3,4] and magnetic hyperthermia cancer therapy.[5–7] A wide range of magnetic NPs, including metals/alloys,[8] metal oxides,[9] ferrites,[10] colossal magnetoresistive (CMR) materials [11] with superior magnetic properties and suitable Curie temperature (T_C), have been synthesized for different biomedical applications. In general, drug targeting by NPs could enhance drug stability, reduce required dosage, minimize side effects and also enhance pharmaceutical effects. Among different NPs, CMR materials, especially those of $La_{0.67}Sr_{0.33}MnO_3$ (LSMO) family are of great biomedical importance, especially for drug delivery applications since they have high T_C ($\geq$360 K) and a large magnetization at room temperature.[12] Kale et al. [13] have reported that Ce-doped and stoichiometry-controlled LSMO NPs are viable heating agents with extremely low cytotoxicity. Although their results related to the cytotoxicity findings are encouraging, more extensive study is required to make these NPs biocompatible. There are few reports where the magnetic NPs have been coated with a biocompatible shell [14] or embedded in a polymer [15] to avoid aggregation and confer biocompatibility.[16] Recently, Soleymani

CONTACT Sunita Keshri s_keshri@bitmesra.ac.in; sskeshri@rediffmail.com

et al. have reported that polymer-coated $La_{0.73}Sr_{0.27}MnO_3$ NPs can have potential applications in cancer hyperthermia therapy and magnetically activated drug delivery.[17] But challenges in current magnetic drug delivery systems include unacceptable coincidental heating of healthy tissue, control of the drug release time as well as the released amount, cytotoxicity and biocompatibility. More extensive work in this direction is required. We have previously reported [18] about the successful synthesis of biocompatible composite of LSMO and hydroxyapatite (HA) particles. In this composite, the NPs of LSMO (of size 50−120 nm) are found to be surrounded by HA particles and acquired a size of 300−600 nm. That work was not extended up to the drug loading and release studies, and T_C of the grown composite sample was less (∼230 K). Moreover, according to few other reports, [19] the particles in the range of 10−100 nm appear to be ideal for biomedical use because they are small enough to penetrate very small capillaries within the body tissues for most effective distribution, ensuring adequate blood circulation times. So, as an advancement of our previous work, in the present study, LSMO NPs of grain size 25−45 nm have been grown and made biocompatible by embedding them in an acrylic interpenetrating polymer network (IPN). In order to study the drug loading and release properties of the grown sample, a test antibiotic, ciprofloxacin, has been loaded into it. The controlled release profile of this drug loaded in the sample has been investigated as a function of time in distilled water as reported in [20]. The main aim of this study is to see the loading and release capacity of the drug loaded in the grown polymer embedded with LSMO NPs and their influence on different microorganisms. Good antibacterial activity has been found against a Gram-positive bacteria, *Bacillus subtilis* (*BS*) and a Gram-negative bacteria, *Salmonella typhi* (*ST*).

2. Experimental

2.1. Synthesis of LSMO NPs

LSMO NPs were prepared by the sol−gel method. In order to prepare a 5 g of LSMO, stoichiometric amount of the nitrate reagents $La(NO_3)_3.6H_2O$ (2.3975 g), $Sr(NO_3)_2$ (0.5775 g) and $Mn(NO_3)_2$ (2.0250 g) were dissolved in distilled water and were mixed with citric acid to prepare a stable solution. Drops of ammonia water were added to the solution to increase its pH value to 7. A gelatin reagent, ethylene glycol, was added to this solution and heated on a hot plate under a constant stirring at 80 °C to eliminate the excess water and to obtain a viscous gel. Citric acid and ethylene glycol were added to the solution of metal nitrates in the following molar ratio: metal nitrate:citric acid:ethylene glycol = 1:5:5. The gel was dried at 250 °C and calcined at 500 °C for 6 h to get the desired powder. The powder thus obtained was pelletized and sintered at 800 °C. In order to verify the crystalline behaviour of the sample, powder X-ray diffraction using Rigaku diffractometer with CuK_α radiation from 10° to 80° with a step size of 0.02° was used. Fourier transform infrared spectroscopy (FTIR) spectra of samples were obtained using an FTIR-8400S instrument (Shimadzu, Kyoto, Japan). A small amount of the grown powder sample was mixed with KBr powder in the ratio 0.5:99.5 and placed into a sample holder, a small stainless steel crucible, for the analysis. The spectrum was scanned in the range of 400−4000/cm at a resolution of 2/cm with scan speed of 64 scan/s and was recorded using IR Solution software (Shimadzu). The morphology of the prepared samples was examined by scanning electron microscopy (SEM) (JEOL, Model: JSM-6390LV; Tokyo, Japan) equipped with energy dispersive X-ray (EDX) spectrometer (Oxford INCA, Model: DCL−7673). The samples were coated using platinum to increase the conductivity of the electron beam. Grain size determination was carried out using a transmission electron microscope (TEM) (model: Philips CM200). Magnetization of the sample was measured at 10 kOe DC field using a vibration magnetometer (Lake Shore, model 7407).

2.2. Synthesis of interpenetrating polymer network embedded with LSMO NPs

Hydrophobic butyl acrylate monomer (CDH, 99.0%) was purified by washing with 2% (1 g in 50 ml water) of sodium hydroxide (CDH, 99.8%) solution, followed by thorough and repeated washings with distilled water to make it alkaline-free. The purified monomer was dried by keeping in contact of anhydrous calcium chloride for 1 h and then stored for 24 h in refrigerator after filtration. To prepare the IPN, poly(butyl acrylate) (PBA) was first formed using a 5 ml of monomer and 2% (0.1 g) initiator, benzoyl peroxide (Bz_2O_2) (CDH, purity 99.9%) by the method of bulk polymerization at 80 °C under inert atmosphere of nitrogen. A gel was thus formed. It was then swollen with the mixture of 5 ml of another monomer, hydrophilic 2-hydroxyethyl acrylate (HEA, Sigma–Aldrich, purity 99.9%), 2% (0.1 g) of Bz_2O_2 and 2% (0.1 g) of crosslinker, ethylene glycol dimethacrylate for 24 h. The LSMO NPs (1.8 mg) were added to this liquid mixture prior to the start of polymerization in order to embed the NPs in the IPN of final weight ~10.302 g. The whole mixture was sonicated for 2 h, followed by heating at 80 °C for another $^1/_2$ h that led to the formation of an acrylic IPN embedded with LSMO NPs. In the present case, a full IPN was formed as both the component polymers were crosslinked by the same crosslinker. The sample, formed in this way, was distilled with boiling ethanol (78 °C) in a glass chamber attached with a condenser having water circulation arrangement. During the distillation process, which continued for 24 h, the unreacted monomers entrapped in the crosslinked polymer got eliminated along with ethanol vapour. The polymer sample was then taken out of this distillation chamber and vacuum dried at 80 °C for 8 h to ensure the removal of last tinge of unreacted monomer. The dried sample was a soft gel-like tacky grey mass; the colour was due to the NPs embedment. This polymer sample embedded with LSMO NPs was used for drug loading and release studies, and also its anti-bacterial activity was tested.

3. Result and discussion

3.1. Characteristic properties

The XRD patterns of LSMO sample are shown in Figure 1(a). The structural analysis was carried out using the 'Checkcell' software and its unit cell was found to match with the rhombohedral structure of $R\overline{3}c$ space group with $a = b = 0.5496$ nm and $c = 1.3365$ nm. The crystallite size and lattice strain of the synthesized sample were found to be ~15 nm and 0.0087, respectively, calculated using the Hall–Williamson formula [21]:

$$\beta \cos\theta = \frac{0.89\lambda}{D} + 4\varepsilon \sin\theta, \tag{1}$$

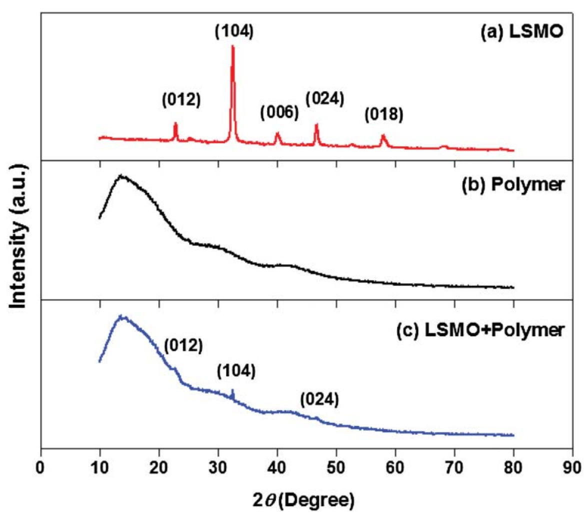

Figure 1. XRD patterns of (a) LSMO NPs, (b) polymer and (c) LSMO-embedded polymer.

where λ is the wavelength of the X-ray radiation ($\lambda = 0.1546$ nm), θ is Bragg's angle, ε is the lattice strain and β is the full width at half-maximum (FWHM). The XRD patterns of the grown polymer and the LSMO-embedded polymer are shown in Figure 1(b) and 1(c), respectively. The characteristic pattern of an amorphous material was observed for the grown acrylic polymer. The XRD pattern of the composite shows a combined pattern of both the phases, confirming that a composite sample was grown successfully.

Figure 2(a)−(c) shows the FTIR spectra of the as-prepared LSMO NPs, polymer and LSMO-embedded polymer, respectively. The first peak of the spectrum of LSMO at $\sim$405 cm^{-1} corresponds to the bending mode (ν_b) of Mn−O−Mn bond angle and the strong absorption peak at $\sim$608 cm^{-1} arises from the stretching mode (ν_s) of Mn−O−Mn bond which involves the internal motion of a change in bond length in MnO_6 octahedra. The peak at $\sim$858 cm^{-1} of the same spectrum is due to the presence of C−O bond of the atmospheric CO_2, whereas the broad bands at 1622 and 3451 cm^{-1} correspond to adsorbed water. The peak at $\sim$1470 cm^{-1} corresponds to unreacted carbonates.[22] The spectrum (Figure 2(b)) of the grown polymer shows the characteristic absorption bands of the C=O group stretching vibration at 1737 cm^{-1}, the characteristic absorption bands of the C−H stretching vibration and the C−H in-plane bending vibration at 2873, 2958 cm^{-1} and 1384, 1450 cm^{-1}, respectively.[23] The other peaks appeared at 752, 848 and 941 cm^{-1} resemble with the peaks observed by Wu et al. [24] for PBA sample. In the FTIR spectrum of LSMO-embedded polymer (Figure 2(c)), the peaks of LSMO phase at $\sim$408 and 608 cm^{-1} were observed along with the major peaks of the polymer. These findings give evidence that acrylate polymerization in presence of the LSMO NPs was taken place without any alteration in reaction mechanism.

The SEM image of LSMO sample is shown in Figure 3(a) from which it is understood that the grains are homogeneously distributed. The EDX pattern (Figure 3(b)) of the 'A' region of this sample demonstrates the presence of the desired elements of LSMO phase by exhibiting their intensity peaks. The spectrum also shows the peaks corresponding to Pt as the surface of the sample was coated by Pt to avoid charging. Figure 3(c) presents the SEM image of LSMO mixed with polymer which shows that the NPs of LSMO are well dispersed in the polymer; the EDX pattern of such region (mentioned by 'B') is shown in Figure 3(d). Both the EDX patterns match well, confirming that the NPs of LSMO are embedded in the polymer. To know the grain size of NPs, we carried out TEM study also; the concerned image is presented in Figure 4(a). The image confirms that the grain size of the LSMO NPs lies in the range of 25−45 nm. The corresponding electron diffraction pattern (Figure 4(b)) indicates that the complex oxide was crystallized perfectly.

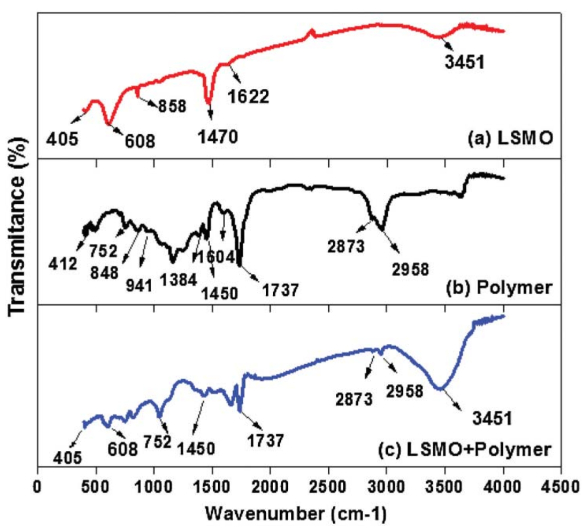

Figure 2. FTIR results of (a) LSMO, (b) polymer and (c) LSMO-embedded polymer.

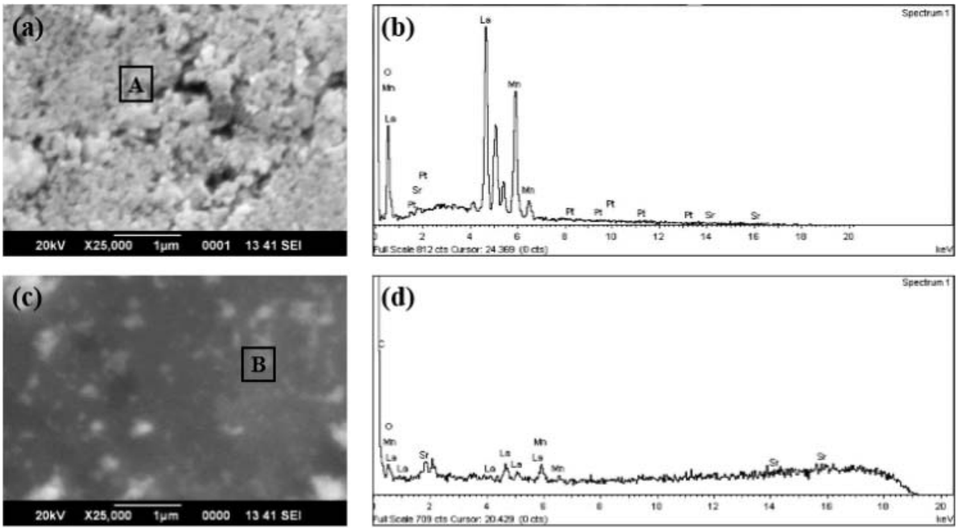

Figure 3. (a) SEM image of LSMO, (b) EDX result of position 'A'; (c) SEM image of LSMO-embedded polymer and (b) EDX result of position 'B'.

In order to study the magnetic properties of these samples, temperature-dependent magnetization, $M(T)$, was measured in the field cooling mode at the applied magnetic field (H) of strength 10 kOe. The results obtained are shown in Figure 5(a) and 5(b). The plots of derivatives of $M(T)$ with respect to T are shown in the insets as a function of temperature, the peak of which defines the Curie temperature (T_C). The $M-T$ data patterns indicate that both the samples undergo a PM to FM transition upon cooling. From these plots, it is evident that T_C of LSMO remains the same ($\sim$355 K) even after embedding it in a polymer network. It is interesting to observe that this result is better than the result obtained for LSMO−HA sample for which T_C was decreased to $\sim$230 K.[18] The field-dependent magnetization, $M(H)$, was also studied at room temperature (RT), and the hysteresis loops are shown in Figure 6(a) and 6(b). The results show that the samples have FM behaviour at RT with reasonably small hysteresis loop and a low coercive field (H_C). From these figures, the saturation magnetic moment (M_S) per unit mass, remanent magnetic moment (M_r) and H_C of the samples were calculated and listed in Table 1. The value of M_S for LSMO NPs is found to be 33.87 emu/g, whereas that of the LSMO-embedded polymer sample is small $(2.44\times10^{-2}$ emu/g) as it includes only 1.8 mg of LSMO in $\sim$10.302 g of IPN.

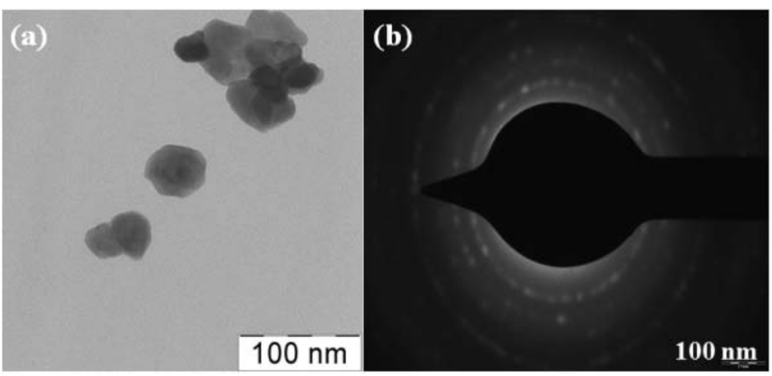

Figure 4. (a) TEM image of LSMO NPs, (b) electron diffraction pattern of the selected area of this sample.

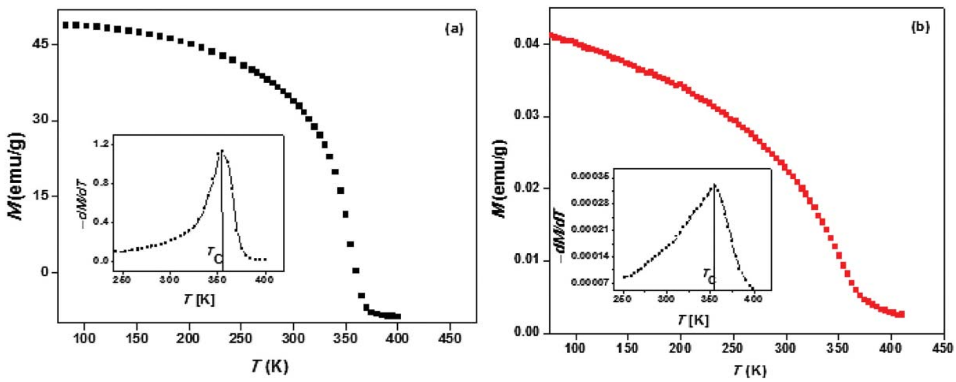

Figure 5. Variation of DC magnetization of (a) LSMO and (b) LSMO-embedded polymer sample under field-cooled condition.

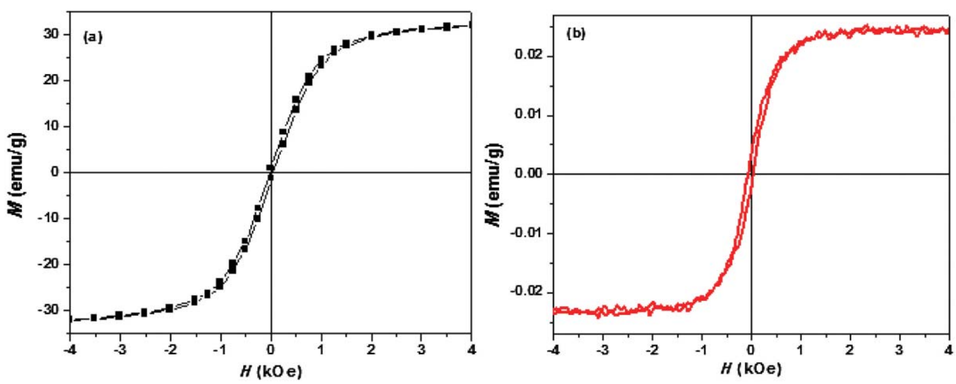

Figure 6. Plots of magnetization versus field of (a) LSMO and (b) LSMO-embedded polymer.

3.2. Drug loading and release properties of LSMO-embedded polymer sample

To investigate the drug loading and release properties of the grown biocompatible sample, LSMO NPs embedded in polymer, we have used the antibiotic ciprofloxacin as the test drug. This antibiotic is well known to provide high concentration of drug at the site of infection with a low systemic toxicity. However, since ciprofloxacin has very short half-life (nearly $3^1/_2$–4 h), multidose therapy of the conventional dosage forms is necessary to get the desired therapeutic effect.[25] Using a controlled drug delivery system, the drug release pattern can be monitored within narrow therapeutic range which leads to minimize the side effect, ensure the safety and improve the efficacy of drugs as well as patient compliance.

Table 1. Some important data obtained from hysteresis loops.

	Sample name	
	LSMO	LSMO embedded in IPN
Saturation field (H_s) (kOe)	4	4
Saturation magnetization (M_s) (emu/g)	33.87	2.44×10^{-2}
Coercive field (H_c) (Oe)	35	41
Remanent magnetization (M_r) (emu/g)	0.72	3.10×10^{-3}

3.2.1. Drug loading or swelling studies

To load drug in the grown sample, a small bead of LSMO-embedded polymer sample of weight 385 mg was placed in a small vial containing 100 ml of distilled water suspended with 2 mg/ml of ciprofloxacin drug. This was shaken at 250 rpm in an orbital shaker incubator (Model – AAH23213U) at 37 °C. The bead was suspended in the medium in such a way that swelling could occur three-dimensionally with water penetrating into the gel bead from all sides. At different time intervals, the bead was gently removed from the hydration medium, surface-dried with filter paper, and reweighed using an analytical balance (Afcosct Electrical Balance, Model – ER-160A). The same bead was used for the experiments of drug loading and release. The drug loading of the gel bead was calculated using the following equation:

$$\text{Amount of drug loading (mg)} = W_f - W_i, \tag{2}$$

where W_i is the initial dry weight of the bead and W_f is the final dry weight of the gel bead after the inclusion of drug. The experiment was performed thrice. The increase in dry weight of the sample was taken as the amount of drug loaded in the sample. A similar method was adopted by several other research groups [26] earlier.

3.2.2. *In vitro* drug release studies

The *in vitro* dissolution study was carried out using United States Pharmacopoeia Apparatus-I dissolution test system (TDT-08 L; Electrolab, India). The dissolution jars were cleaned with a mild detergent and then rinsed with distilled water and dried at room temperature. The jars were filled up with 900 ml of distilled water. The medium of the jars was maintained at (37 ± 0.5) °C and stirred at 75 rpm. In one of these jars, 385.00 mg of test sample loaded with 21.83 mg of drug was introduced. Volumes of 5 ml were withdrawn from this jar at specified time intervals such as 0, 1, 2, 3, 4, 5, 6, 7 and 8 h using a syringe. These nine samples were transferred immediately to clean, dried and labelled test tubes. The absorbance of each sample was measured at 275 nm using UV–visible spectrophotometer. To get the concentration of release drug, the data were compared with the absorbance data of ciprofloxacin dissolved in distilled water, obtained using the same light source. The result is presented in Figure 7(a) which shows an excellent linearity with the coefficient of determination, $R^2 = 0.9979$. The result matches well with the previous reports.[27] The concentration of drug released was calculated as

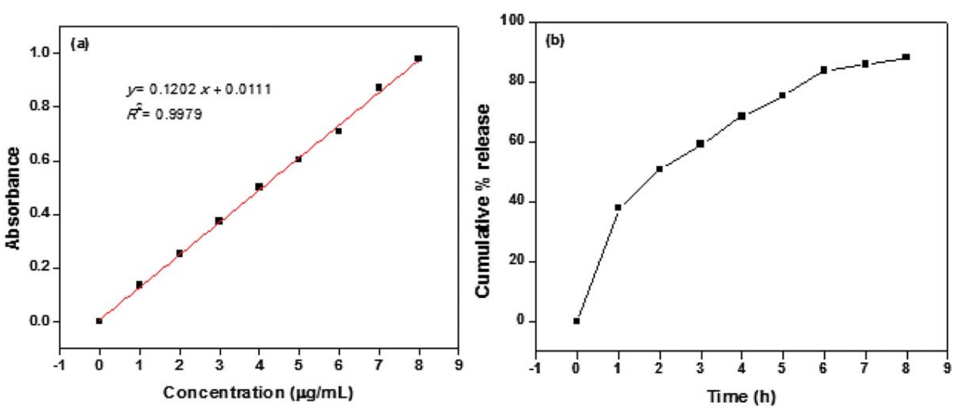

Figure 7. (a) Absorbance behaviour of different concentrations of ciprofloxacin in water and (b) cumulative % release versus time plot for ciprofloxacin loaded in polymer embedded with LSMO NPs.

Table 2. MIC values of the grown LSMO-embedded polymer sample, loaded with ciprofloxacin for different strains of bacteria (MIC value of ciprofloxacin is 0.78 μg/ml).

Microorganisms	Bacteria name	Bacterial strains number	MIC value (μg/ml)
Gram-positive bacteria	*Staphylococcus aureus*	NCIM 2901	1.56
	Bacillus subtilis	MTCC 441	0.78
Gram-negative bacteria	*Escherichia coli*	NCIM 2810	12.50
	Pseudomonas aeruginosa	NCIM 2036	3.13
	Salmonella typhi	NCIM 2501	0.78
	Klebsiella pneumonia	MTCC 3384	12.50

follows:

$$\text{Concentration of drug released}\left(\mu\frac{\text{g}}{\text{ml}}\right) = \frac{(\text{Absorbance} - \text{intercept})}{\text{Slope of absorbance vs. concentration curve of the pure drug dissolved in distilled water}}. \tag{3}$$

The amount of drug released and cumulative percentage release were calculated using the following equations, as mentioned in [28]. The sample was not diluted further and its dilution factor was considered as 1.

$$\text{Amount of drug released (mg) in 900 ml of solution} = \frac{\text{Concentration }\left(\frac{\mu\text{g}}{\text{ml}}\right)\times\text{dissolution bath volume (ml)}\times\text{dilution factor}}{1000}. \tag{4}$$

$$\text{Cumulative percentage release (\%)} = \frac{\text{Amount of drug released (mg)}}{\text{Amount of drug loaded (mg)}}\times 100. \tag{5}$$

Three sets of each sample, collected at different time intervals, were taken to have the average calculation of cumulative percentage release. It is interesting to note that after 8 h, an amount of ~90% from the loaded drug was released and the time-dependent cumulative percentage release is presented in Figure 7(b).

3.3. Effects of the drug loaded in LSMO-embedded polymer sample on different bacteria

We have studied the minimum inhibitory concentration (MIC) of the grown LSMO-embedded polymer sample, loaded with ciprofloxacin for different bacteria. The MIC amounts the lowest concentration of antibacterial that will inhibit the visible growth of a microorganism after overnight incubation. The microorganisms which have been selected for this study are as follows: Gram-positive bacteria – *Staphylococcus aureus* (*SA*) and *Bacillus subtilis* (*BS*), and Gram-negative bacteria – *Escherichia coli* (*EC*), *Peudomonas aeruginosa* (*PA*), *Salmonella typhi* (*ST*) and *Klebsiella pneumonia* (*KP*). The obtained results are listed in Table 2, from which results it is understood that in case of *BS* and *ST* bacteria, the grown LSMO-embedded polymer sample, loaded with ciprofloxacin, has got an equally good antibacterial activity like simple ciprofloxacin. As compared to the MIC value of ciprofloxacin (0.78 μg/ml), the MIC value of ciprofloxacin loaded in the sample is same for *BS* (Gram positive) and *ST* (Gram negative). For other two bacteria, *SA* and *PA*, the MIC values are reasonably acceptable. However, that for *EC* and *KP* is high. Such work carries new information in the field of drug loading and release applications of manganites and demands more extended study in this direction.

4. Conclusions

The present paper contains a thorough report on the synthesis and characteristic properties of LSMO NPs embedded in polymer network. The drug loading and release properties of the grown sample was studied for an antibiotic, ciprofloxacin. We carried out this investigation with an intention to develop biocompatible magnetic (LSMO) NPs and to check their ability of drug loading and release. From the measurement of DC magnetization, it was observed that the grown polymer embedded with LSMO sample exhibits magnetic behaviour similar to that of LSMO without any significant change in T_C. It also preserves the hysteresis behaviour of the parent sample with almost the same value of coercive field, but with lower magnetic moment. The drug loading and release experiments using ciprofloxacin showed that after 8 h, an amount of ~90% from the drug loaded in the grown LSMO-embedded polymer was released. The MIC value of ciprofloxacin loaded in the grown sample was studied for few Gram-positive and Gram-negative bacteria. The result is encouraging and as good as ordinary ciprofloxacin for some of the bacteria strains. Such sample may be used for magnetically activated drug delivery which implies that when reaching the intended diseased site in the body, the drug carried by this composition can be released. It needs to be mentioned that the focus of this work is on the drug loading and release studies of this sample. Obviously, few other challenges are there in order to release the drug in the targeted position with fewer amounts of side effects. More work is required in this direction.

Acknowledgments

The authors are thankful to the members of Central Instrumentation Facility Lab, BIT for FTIR and SEM measurements. XRD work of this study was performed at UGC-DAE Consortium for Scientific Research, Indore; Dr Mukul Gupta is acknowledged for supporting this work. Associate Prof. S.G. Pampalia, Department of Pharmaceutical Science and Technology, BIT is acknowledged for providing the test drug. The authors are also thankful to the members of the Collective Use Centre of the Lomonosov Moscow State University, Russia for providing TEM facility.

Disclosure statement

A new process of embedding CMR NPs in IPN polymer is reported.

Funding

The present work is supported by Department of Science and Technology (DST), India through the DST-RFBR project [P-115, 2012].

References

[1] Singh A, Sahoo SK. Magnetic nanoparticles: a novel platform for cancer theranostics. Drug Discov Today. 2014;19:474–481.
[2] Liberti PA, Rao CG, Terstappen LWMM. Optimisation of ferro fluids and protocols for the enrichment of breast tumor cells in blood. J Magn Magn Mater. 2001;225:301–307.
[3] Worden M, Bruckman MA, Kim M-H, et al. Aqueous synthesis of polyhedral 'brick-like' iron oxide nanoparticles for hyperthermia and T_2 MRI contrast enhancement. J Mater Chem B. 2015;3:6877–6884.
[4] Kulkarni MV, Bodas D, Paknikar MK. Lanthanum strontium manganese oxide (LSMO) nanoparticles: a versatile platform for anticancer therapy. RSC Adv. 2015;5:60254–60263.
[5] Uskoković V, Kosak A, Drofenik M. Silica-coated lanthanum–strontium manganites for hyperthermia treatments. Mater Lett. 2006;60:2620–2622.
[6] Haghniaz R, Umrani RD, Paknikar KM. Temperature-dependent and time-dependent effects of hyperthermia mediated by dextran-coated: in vitro studies. Int J Nanomed. 2015;10:1609–1623.
[7] Solopan S, Belous A, Yelenich A, et al. Nano hyperthermia of malignant tumors. Lanthanum–strontium manganite magnetic fluid as potential inducer of tumor hyperthermia. Exp Oncol. 2011;33:130–135.
[8] Cherukuri P, Glazer ES, Curley SA. Targeted hyperthermia using metal nanoparticles. Adv Drug Deliv Rev. 2010;62:339–345.

[9] Yin ZF, Wu L, Yang HG, et al. Recent progress in biomedical applications of titanium dioxide. Phys Chem Chem Phys. 2013;14:4844−4858.
[10] Doaga A, Cojocariu AM, Amin W, et al. Synthesis and characterizations of manganese ferrites for hyperthermia applications. Mater Chem Phys. 2013;143:305−310.
[11] Manh DH, Phong PT, Nam PH, et al. Structural and magnetic study of $La_{0.7}Sr_{0.3}MnO_3$ nanoparticles and AC magnetic heating characteristics for hyperthermia applications. Physica B. 2014;444:94−102.
[12] Horiki M, Nakagawa T, Seino S, et al. Heating ability of La−Sr−Mn−Cu perovskite spheres under an alternating current magnetic field for magnetic hyperthermia mediators. J Magn Magn Mater. 2013;329:49−52.
[13] Kale SN, Arora S, Bhayani KR, et al. Cerium doping and stoichiometry control for biomedical use of nanoparticles: microwave absorption and cytotoxicity study. Nanomedicine. 2006;2:217−221.
[14] Kumar SSR, Mohammad CF. Magnetic nanomaterials for hyperthermia-based therapy and controlled drug delivery. Adv Drug Deliv Rev. 2011;63:789−808.
[15] Li J, Qu Y, Ren J, et al. Magnetocaloric effect in magnetothermally responsive nanocarriers for hyperthermia-triggered drug release. Nanotechnology 2012;23:505706.
[16] Yavuz MS, Cheng Y, Chen J, et al. Gold nanocages covered by smart polymers for controlled release with near-infrared light. Nat Mater. 2009;8:935−939.
[17] Soleymani M, Edrissi M, Alizadeh MA. Thermosensitive polymer-coated $La_{0.73}Sr_{0.27}MnO_3$ nanoparticles: potential applications in cancer hyperthermia therapy and magnetically activated drug delivery systems. Polym J. 2015;47:797−801.
[18] Keshri S, Kumar V, Wisniewski P, et al. Synthesis and characterization of LSMO manganite-based biocomposite. Phase Transit. 2014;87:468−476.
[19] Bhayani KR, Kale SN, Arora S, et al. Protein and polymer immobilized nanoparticles for possible biomedical applications. Nanotechnology. 2007;18:345101−345108.
[20] Gupta R, Bajpai AKJ. Magnetically guided release of ciprofloxacin from superparamagnetic polymer nanocomposites. Biomater Sci Polym. 2011;22:893−918.
[21] Mote VD, Purushotham Y, Dole BN. Williamson−Hall analysis in estimation of lattice strain in nanometer-sized ZnO particles. J Theor Appl Phys. 2012;6:1−8.
[22] Yang W-D, Chang Y-H, Huang S-H. Influence of molar ratio of citric acid to metal ions on preparation of materials via polymerizable complex process. J Eur Ceram Soc. 2005;25:3611−3618.
[23] Wang G. Synthesis of poly(*n*-butyl acrylate) homopolymers by activators generated by electron transfer (AGET) ATRP using $FeCl_3.6H_2O$/succinic acid catalyst. Iran Poly J. 2011;20:931−938.
[24] Wu X, Shi G. Synthesis of a carboxyl-containing conducting oligomer and non-covalent sidewall functionalization of single-walled carbon nanotubes. J Mater Chem. 2005;15:1833−1837.
[25] Begg EJ, Robson RA, Saunders DA, et al. The pharmacokinetics of oral fleroxacin and ciprofloxacin in plasma and sputum during acute and chronic dosing. Br J Clin Pharmacol. 2000;49:32−38.
[26] Kiran K, Goswami S, Sharma PP, et al. Study of drug transport phenomenon of acrylic IPNs embedded with iron oxide nanoparticles. Int J Polym Mater Polym Biomater. 2012;62:509−516.
[27] Laignier Cazedey EC, Nunes Salgado HR. Spectrophotometric determination of ciprofloxacin hydrochloride in ophthalmic solution. Adv Anal Chem. 2012;2:74−79.
[28] The Indian Pharmacopoeia, Government of India, Ministry of health and family welfare, Controller of publication, New Delhi, Volume II, 1996;A80−A84.